Actomyosin forces and the energetics of red blood cell invasion by the malaria parasite *Plasmodium falciparum*

Thomas C. A. Blake[1], Silvia Haase[1] and Jake Baum[1,*]

[1]Department of Life Sciences, Imperial College London, South Kensington, London SW7 2AZ, UK.

*Correspondence to:

Jake Baum (jake.baum@imperial.ac.uk), Department of Life Sciences, Imperial College London, Exhibition Road, South Kensington, London, SW7 2AZ, UK. Tel. +44 (0)20 75945420

Short title: Myosin motors in malaria red cell entry

Supplementary Information

Includeed in this file:

Supplementary Figures S1-S3

Supplementary Video S4-S8 legends

Supplementary Tables S1-S2

Supplementary Figures

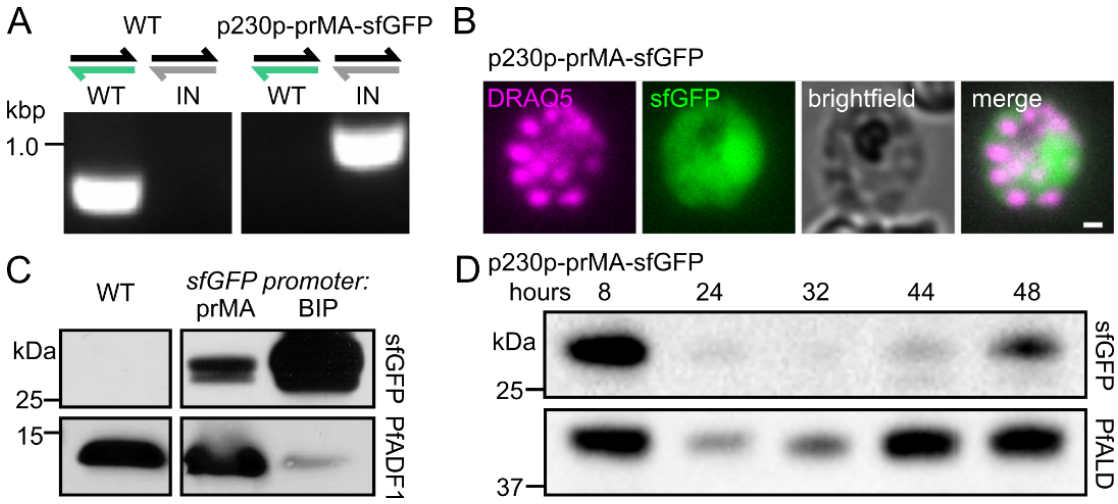

Figure S1: Validation of *Pfmyoa* promoter system at the *p230p* locus

A Exchanging the constitutive *BIP* promoter for the *Pfmyoa* promoter produced p230p-prMA-sfGFP parasites. Genotyping PCR showed a complete loss of the WT *p230p* locus (green half arrow) and gain of the integrated locus (IN, grey half arrow). **B** Live fluorescence microscopy of p230p-prMA-sfGFP schizont showing DNA (DRAQ5, magenta) and cytosolic sfGFP expression. **C** Western blot of p230p-prMA-sfGFP parasites confirming sfGFP expression, although at a lower level than constitutive p230p-BIP-sfGFP. **D** Western blot of p230p-prMA-sfGFP parasite lysate, normalised by total protein level, at different stages of the asexual life cycle. Strong expression of sfGFP was present in late schizonts and early rings only, as expected for the *Pfmyoa* promoter, while control protein *P. falciparum* aldolase (PfALD) levels dip slightly in trophozoite stages.

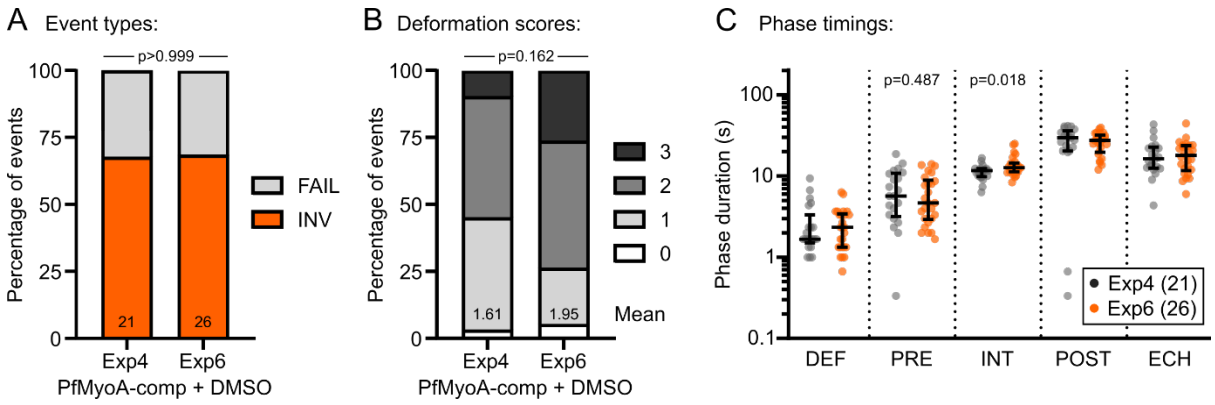

Figure S2: Video microscopy of PfMyoA-comp, broken down by biological repeat to assess consistency

A To assess the consistency of the two biological repeats, each two technical repeats, performed for each line, since the statistical tests assume that all events are independent, PfMyoA-comp + DMSO was chosen as an example where both repeats (Exp4 and Exp6) had similar numbers of events. The proportion of successful invasion events in both experiments was the same (p>0.999, Fisher's exact test, comparing pooled failures to Type A). **B** Comparing the deformation scores across the two experiments showed some differences, but not significant (p=0.162, chi square test). **C** Comparing the distributions of each phase duration across the two experiments showed only small differences. The duration of internalisation was significantly higher in Exp6, but the difference was small (11.7 s to 12.7 s). Bars show median and interquartile range. Significance assessed for each phase by Mann-Whitney test, shown when p<0.5.

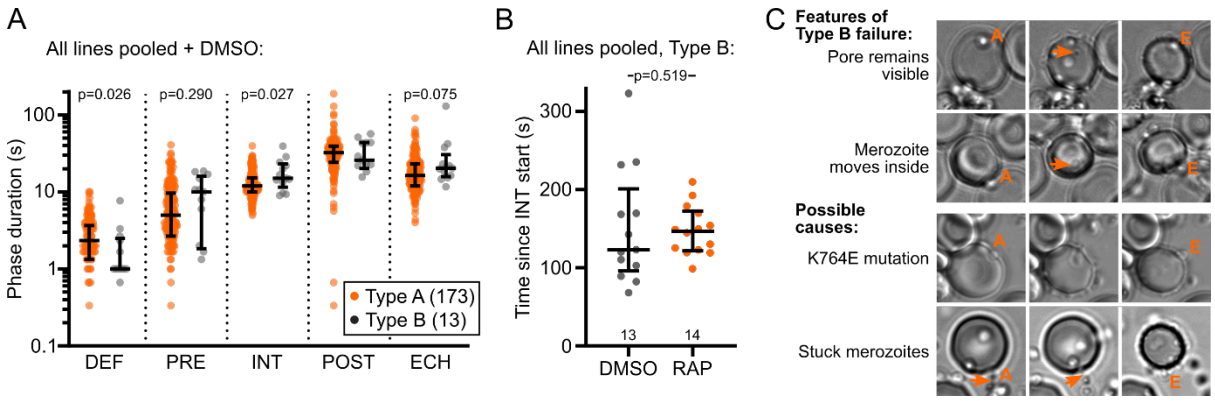

Figure S3: Type B events show slower internalisation

A From all lines after DMSO treatment, comparing Type A events to Type B events shows a significantly shorter deformation period and slower internalisation, with a trend to a longer pause before internalisation, consistent with either a merozoite producing less force or an RBC providing more resistance to invasion. Bars show median and interquartile range. Significance assessed for each phase by Mann-Whitney test, shown when $p<0.5$. **B** Comparing Type B failures from all DMSO- or RAP-treated lines shows no difference in the delay from start of internalisation to merozoite ejection. Bars show median and interquartile range. Significance assessed by Mann-Whitney test. **C** Example images of Type B failure where the invasion pore remained visible, hence not resealed (A= attachment, E= ejection); the incompletely-internalised merozoite continuing to move in a swirling pattern within the invagination; an ejection from PfMyoA-K764E after RAP treatment, where Type B failure was more common; and an event where resealing after internalisation was prevented by tethering to a sister merozoite.

Supplementary Videos

Video S4: PfMyoA-cKO merozoites attach but do not deform or internalise

An example of a RAP-treated PfMyoA-cKO merozoite being stably attached (A) but neither deforming nor being internalised before echinocytosis (E), as expected from the absence of the PfMyoA motor. Time indicated in seconds, scale bar 2 µm.

Video S5: PfELC-cKO merozoites deform but do not internalise

An example of a RAP-treated PfELC-cKO merozoite showing attachment (A) and deformation (D) but no internalisation before echinocytosis (E), indicative of a weakened, but present, PfMyoA motor. Time indicated in seconds, scale bar 2 µm.

Video S6: PfMyoA-K764E merozoites are more often ejected after internalisation

An example of a RAP-treated PfMyoA-K764E merozoite showing apparently normal attachment (A), deformation (D) and internalisation (I), before the merozoite was subsequently ejected (arrowhead), after echinocytosis (E) was completed. This suggests a weakened PfMyoA motor, but the merozoite appeared to remain motile while emerging from the RBC. Time indicated in seconds, scale bar 2 µm.

Video S7: PfMyoB-cKO merozoites take longer to initiate internalisation

An example of a RAP-treated PfMyoB-cKO merozoite showing apparently normal attachment (A), deformation (D) and internalisation (I), before echinocytosis (E). On average the loss of PfMyoB delayed the start of internalisation. Time indicated in seconds, scale bar 2 µm.

Video S8: *P. falciparum* merozoites exhibit swirling motility before and during invasion

An example of a RAP-treated PfMyoB-cKO merozoite (though WT merozoites behaved similarly), demonstrating a swirling motion (arrowhead) after attachment (A), before internalisation (I) and echinocytosis (E). This matches observations of *P. knowlesi* merozoites, which glide in a corkscrew motion on a substrate (Yahata *et al*, 2020). Time indicated in seconds, scale bar 2 µm.

Supplementary Tables

Table S1: Oligonucleotides used in this study for genotyping PCR and sequencing

#	Locus	Part	Sequence	Source
1	*p230p*	WT[a]/IN[b]-F	ACCATCAACATTATCGTCAG	Ashdown *et al, in press*
2	*p230p*	WT-R	TCTTCATCAGCCTGGTAAC	Ashdown *et al, in press*
3	*p230p*	IN-R	CATTTACACATAAATGTCACAC	Ashdown *et al, in press*
4	PfMyoA-K764E	IN-F	GTTCATTGATTGGATCTCAGTTC	This study
5	PfMyoA-K764E	IN-R	GGATACGAGCCAGCATAGTC	This study
6	PfMyoA-cKO	IN/EX[c]-F	GGTCGTTTCATGCAGTTGGT	(Robert-Paganin *et al*, 2019)
7	PfMyoA-cKO	IN-R	GCCAGCCACGATAGCCGCGCTGCCTCGTCCTGCAGT TCATTCAGGGCACCGGACAGGTCG	(Robert-Paganin *et al*, 2019)
8	PfMyoA-cKO	EX-R	ACCTTCACCCTCTCCACTGAC	(Robert-Paganin *et al*, 2019)
9	PfMyoB-cKO	WT/IN/EX-F	ATGGGATCGAAAAGGGTGGT	This study
10	PfMyoB-cKO	WT-R	TCCATGATCACTCGTCCTCAC	This study
11	PfMyoB-cKO	IN-R	AAGTCTCCACAATTGATAAAGAG	This study
12	PfMyoB-cKO	EX-R	TTATTTGTACAGTTCATCCATACC	This study
13	pDC2-p230p-BSD	Seq[d] (*bsd*)	TTTTTGTAATTTCTGTGTTTATG	This study
14	pDC2-generic	Seq (gRNA)	AAGCACCGACTCGGTGCCAC	Marcus Lee
15	p230p-prMA-sfGFP	Seq (*sfgfp*)	TGAACCATACGGGTTGTTG	This study
16	p230p-prMA-MyoA	Seq (*myoa)*	CTCCTGGAGCCAAGCAC	This study

[a]WT = wild type locus, [b]IN = integrated locus, [c]EX = excised locus, [d]Seq = sequencing

Table S2: Oligonucleotides used in this study for cloning PCR and guide RNAs

#	Construct	Part	Sequence	Source
17	pDC2-p230p-BSD	BSD-F	ATATCCATGGCCAAGCCTTTGTCTCAAGAAGAATCC	This study
18	pDC2-p230p-BSD	BSD-R	ATATCCGCGGTTAGCCCTCCCACACATAAC	This study
19	p230p-prMA-sfGFP	prMA-F	ATATCCGCGGAGCATGCACAATTAAGAAGACG	This study
20	p230p-prMA-sfGFP	prMA-R	ATATGCTAGCTTTTTTTTTTTTTTTATAAATATGAA AAG	This study
21	p230p-prMA-PfMyoA	MyoA-F	CTTTTCATATTTATAAAAAAAAAAAAAAAGCTAGCA TGGCCGTTACCAACG	This study
22	p230p-prMA-PfMyoA	MyoA-R	GATATTTACTTATTTATTTTATTCTGCATATTTAAA AATCCTGCAGTTAGACCGCATAATCCGG	This study
23	p230p-prMA-K764E	SDM[a]-F	GCAAGAGGGTGCTGAAATTTTAACAAAAATAC	This study
24	p230p-prMA-K764E	SDM-R	ATTTTTGTTAAAATTTCAGCACCCTCTTGC	This study
25	p230p-prMA-S19A	SDM-F	GTGAGGAGAGTAGCTAACGTGGAGG	This study
26	p230p-prMA-S19A	SDM-R	CAAAAGCCTCCACGTTAGCTACTCTCCTC	This study
27	p230p-prMA-DN	MyoA-F	CTTTTCATATTTATAAAAAAAAAAAAAAAGCTAGCA TGAACGTGGAGGCTTTTGATAAATC	This study
28	pUC-PfMyoB-CK	HR[b]-F	CAGTCACGACGTTGTAAAACGACGGCCAGTGAATTC TTAGAGAATTTCATAGGTATTTTGG	This study
29	pUC-PfMyoB-CK	HR-R	TGCGTAATCCGGTACATCATATGGGTACATTTCATG CTCTTTTATATATTTGTACTTAC	This study
30	pUC-PfMyoB-CK	SF[c]-F	ATGTACCCATATGATGTACCG	This study

31	pUC-PfMyoB-CK	SF-R	TTATTTGTACAGTTCATCCATACC	This study
32	pUC-PfMyoB-CK	3UTR[d]-F	ACGCATGGTATGGATGAACTGTACAAATAACTCGAG AAATCGGGAAAATAAAATGG	This study
33	pUC-PfMyoB-CK	3UTR-R	TATGACCATGATTACGCCAAGCTTGCATGCCTGCAG GTCGTCCCAATCATTTTTC	This study
34	pDC2-p230p-hDHFR	gRNA[e]-F	TATTAGGCTGATGAAGACATCGGG	Ashdown *et al, in press*
35	pDC2-p230p-hDHFR	gRNA-R	AAACCCCGATGTCTTCATCAGCCT	Ashdown *et al, in press*
36	pDC2-pfmyob-hDHFR-1	gRNA-F	TATTGTATAAGATAGGAAAAAGCA	This study
37	pDC2-pfmyob-hDHFR-1	gRNA-R	AAACTGCTTTTTCCTATCTTATAC	This study
38	pDC2-pfmyob-hDHFR-2	gRNA-F	TATTGTAGAAGCATTTGACAAAAG	This study
39	pDC2-pfmyob-hDHFR-2	gRNA-R	AAACCTTTTGTCAAATGCTTCTAC	This study

[a]SDM = site-directed mutagenesis, [b]HR = homology region, [c]SF = synthetic fragment, [d]3UTR = 3' un-translated region, [e]gRNA = guide RNA.